

## Supplementary material

### Unexpected reduction in thermal conductivity observed in graphene/h-BN heterostructure

Zhang WU<sup>1</sup>, Rumeng LIU<sup>1,a</sup>, Ning WEI<sup>2</sup>, Lifeng WANG<sup>1</sup>

<sup>1</sup>State Key Laboratory of Mechanics and Control for Aerospace Structures,  
Nanjing University of Aeronautics and Astronautics, 210016 Nanjing, PR China

<sup>2</sup>Jiangsu Key Laboratory of Advanced Food Manufacturing Equipment and Technology,  
Jiangnan University, 214122 Wuxi, PR China

#### I. Temperature-dependence of thermal conductivity

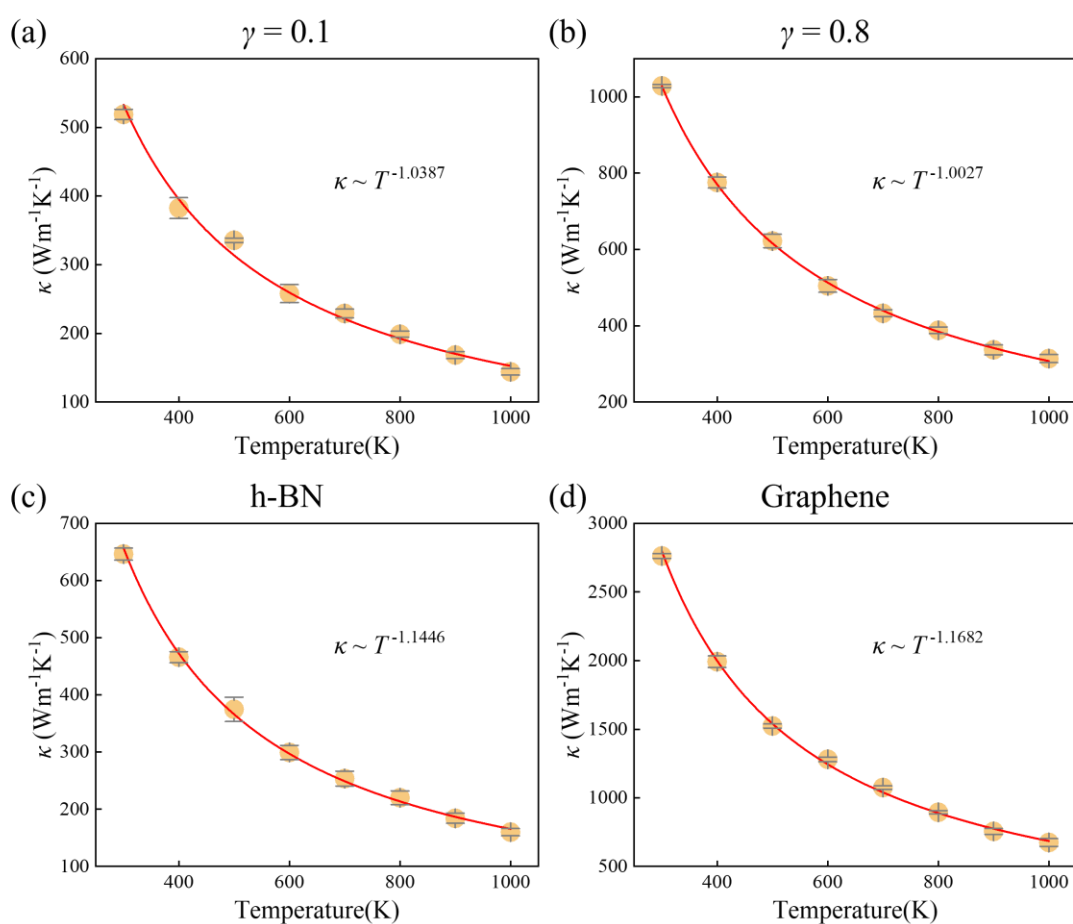


Fig. S1 Thermal conductivity of different temperature with (a)  $\gamma = 0.1$ , (b)  $\gamma = 0.8$ , (c) h-BN and (d) graphene

<sup>a</sup> Author to whom correspondence should be addressed. Electronic mail: [liurumeng@nuaa.edu.cn](mailto:liurumeng@nuaa.edu.cn)

We calculate the thermal conductivity of nanoribbons at different temperature using HNEMD method when  $\gamma = 0.1$  and  $\gamma = 0.8$  with 2 interfaces. The results indicate that the heterostructure still exhibits temperature dependency, aligning with the Eucken-Debye law ( $\kappa \sim T^{-\alpha}$ ). In order to facilitate the comparison, we simultaneously used the same method to calculate the thermal conductance of pure graphene and h-BN at different temperatures. It can be seen from the comparison that, compared with pure graphene and h-BN, the introduction of heterojunction interface increases the anharmonicity of phonons, reduces the thermal conductance, and weakens the temperature dependence, resulting in a decrease in the value of  $\alpha$ .

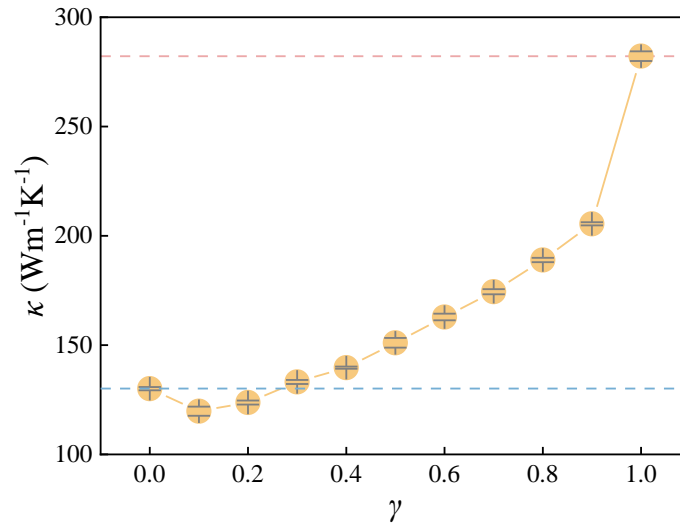


Fig. S2 Relationship between  $\kappa$  and  $\gamma$  at 600K

Next, we calculate the thermal conductivity of nanoribbons at different  $\gamma$  using NEMD method at 600K. Notably, akin to the phenomenon at 300K, it is apparent that for small  $\gamma$  values, the thermal conductivity is lower compared to that of pure h-BN. This indicates that the trend does not disappear with the change of temperature.

## II. Strain effect on thermal conductivity

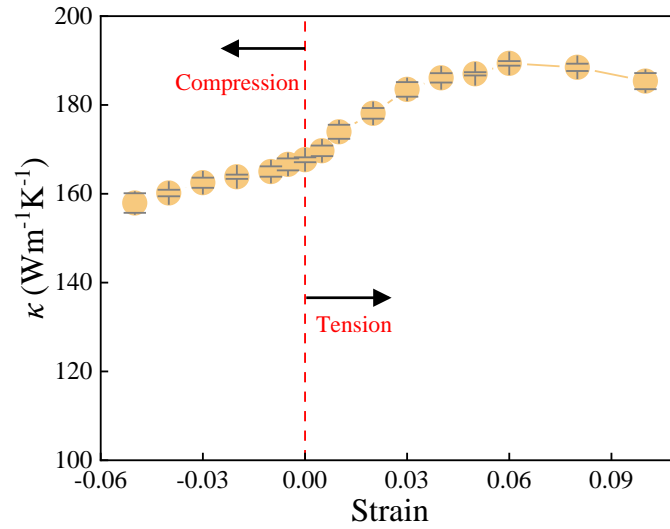


Fig. S3 Relationship between  $\kappa$  and strain at 300K when  $\gamma = 0.1$

We calculate the thermal conductivity of nanoribbons under different strain using NEMD method at 300K with  $\gamma = 0.1$ . The results indicate that the thermal conductivity indeed undergoes significant modulation under different tensile strains. When the heterojunction experiences tensile strain in the direction of heat flux, the thermal conductivity initially increases and then decreases with the increasing strain. Conversely, when subjected to compressive strain in the direction of heat flux, the thermal conductivity decreases with the increasing strain. The findings further validate your insight that mechanical strain is an effective means to manipulate the physical properties of such nanostructures.

### III. Size effect in NEMD simulations

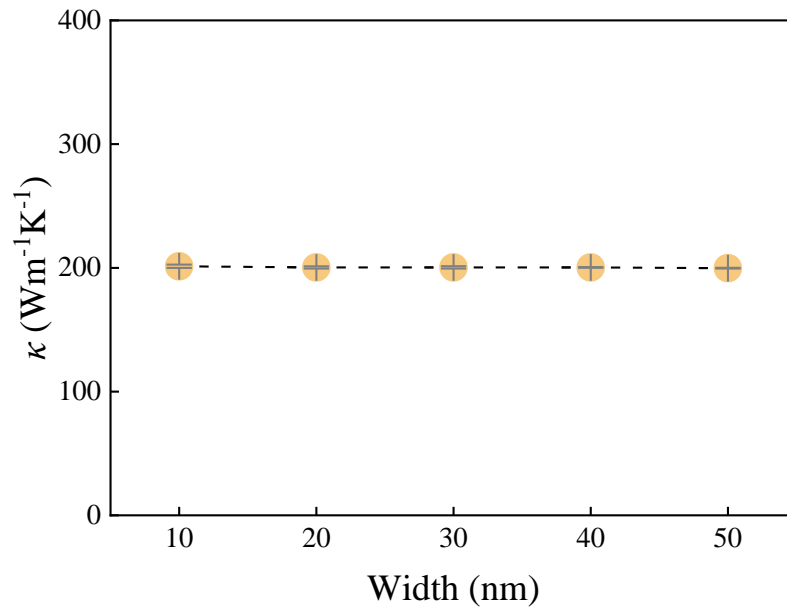


Fig. S4 Relationship between  $\kappa$  and width at 300K when  $\gamma = 0.5$

We calculate the thermal conductivity of nanoribbons with different widths using NEMD method. The models are the heterostructure with  $\gamma = 0.5$  and two interfaces. The plot of thermal conductivity against width intuitively illustrates that changes in width do not have a significant impact on thermal conductivity.

#### IV. Extension of thermal conductivity results

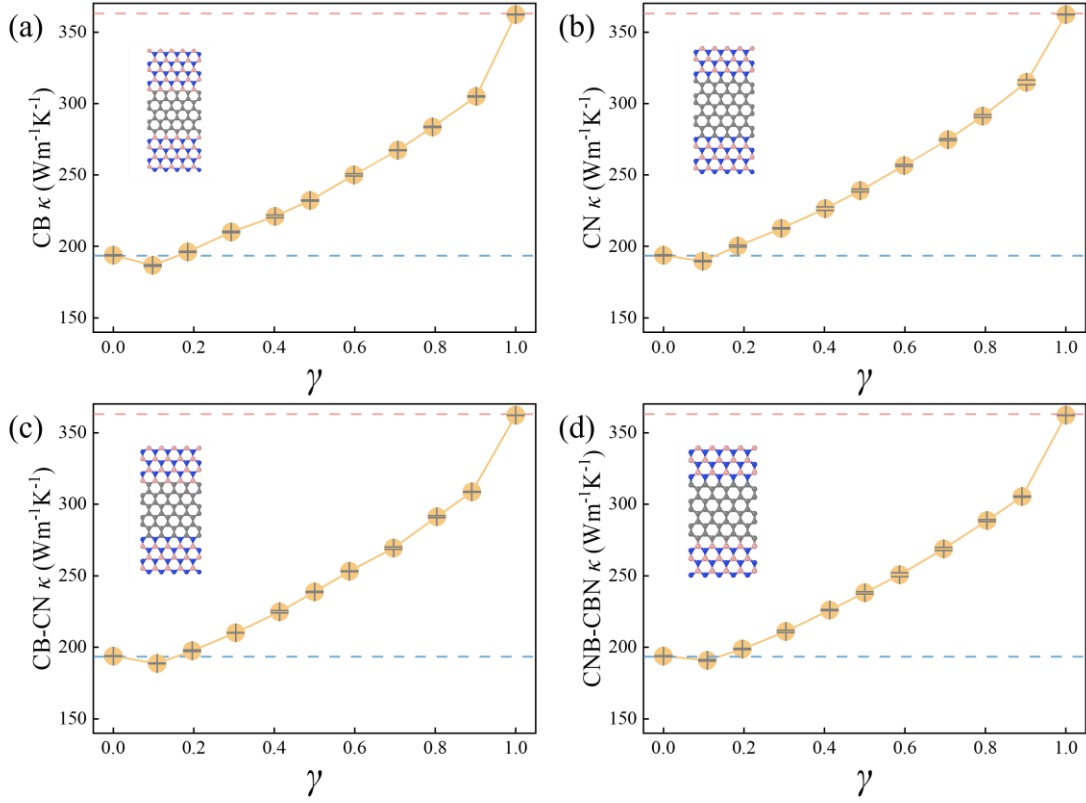


Fig. S5 Thermal conductivity of different  $\gamma$  with (a) CB type interface atoms, (b) CN type interface atoms, (c) CB-CN type interface atoms, and (d) CNB-CBN type interface atoms. C, N, and B represent carbon atoms, nitrogen atoms, and boron atoms, respectively.

We calculate the thermal conductivity of nanoribbons with different atomic bonding types on the interfaces using the NEMD method. The results indicate that the thermal conductivity of zigzag-formed parallel heterojunctions can be lower than that of h-BN when  $\gamma = 0.1$ . Moreover, the different types of chemical bonds between atoms on the interface also affect thermal conductivity.

## V. The calculation and result details in HNEMD simulations

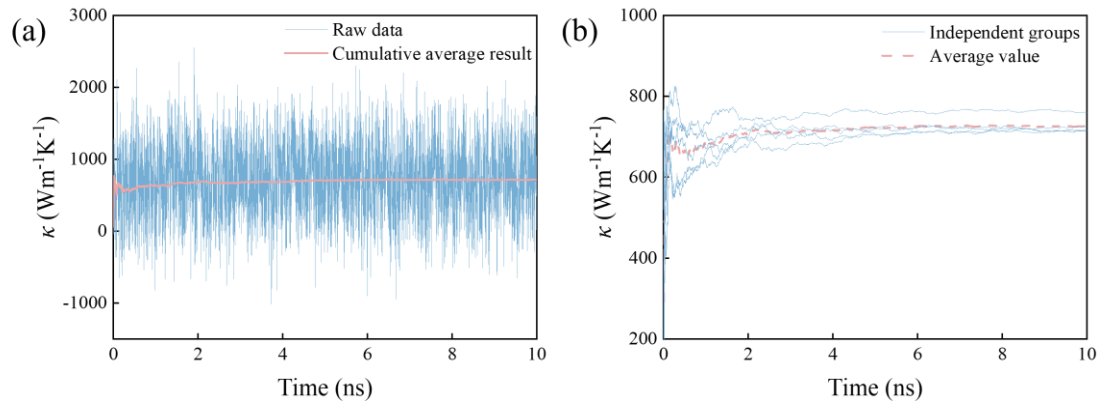


Fig. S6 (a) Running thermal conductivity results versus time before and after the cumulative averaging treatment (b) Results of five independent simulations and their averages. (In this simulation, we set  $F_e = 0.1 \mu\text{m}^{-1}$ .)

We use HNEMD method to calculate the thermal conductivity of the heterostructure with  $\gamma = 0.5$  at 2 interfaces at 300K. From the results, the thermal conductivity results converge well with increasing time under our settings.